Filtering Technique for Stabilization of Marching-on-in-Time Method

Jaroslav LÁČÍK

Dept. of Radio Electronics, Brno University of Technology, Purkynova 118, 612 00 Brno, Czech Republic

lacik@feec.vutbr.cz

Abstract. *In this paper, digital filters are used for the stabilization of the marching-on-in-time (MOT) method. A methodology of designing a proper filter using optimization techniques is proposed here. Since the proposed procedure considers the important part of the spectrum of the excitation signal, the designed filter does not degrade the accuracy of the MOT method. Further, the procedure for the efficient stabilization of the MOT method by a set of filters is proposed and verified on the examples.*

Keywords

Time domain electric field integral equation, method of moments, marching on in time method, stability, filtering technique.

1. Introduction

For the broadband analysis of electromagnetic radiation and scattering, the time domain integral equations (TDIE) can be solved. For their numerical solution, the marching-on-in-time (MOT) method [1], or the marching-on-in-degree (MOD) method [2] which is sometimes called marching-on-in-order (MOO) method, can be applied.

Whereas the finite difference delay modeling (FDDM) method [3] is unconditionally stable, the MOT method suffers from the late time oscillations. MOD method is unconditionally stable also. However, the unconditionally stable approaches usually exhibit lower efficiency and higher memory demands compared to the conventional MOT approaches. In addition, the unconditionally stable algorithms are hardly applicable to the analysis of electrically large structures.

In the literature, several approaches have been published to stabilize a conventional MOT method. The published approaches consist in using implicit time stepping schemes [1], [4], using special kinds of temporal basis functions [5], [6], averaging currents in time [7], or averaging currents in time and space [8], or filtering the current in time by a finite impulse response (FIR) filter [9]. Although these techniques are able to improve the stability of the MOT method, these improvements are not generally valid. In addition, the averaging/filtering techniques usually decrease the accuracy of the MOT method [7]–[9]. In case of applying the filtering technique [9], an appropriate order of a filter is difficult to be chosen.

The paper is focused on the improvement of the filtering technique to become an accurate and efficient tool in the elimination of the late time oscillations. The proposed technique is demonstrated on the solution of the time domain electric field integral equation (TD-EFIE).

The paper is organized as follows. Section 2 presents the TD-EFIE formulation and the MOT method. Section 3 discusses the stabilization of the MOT method by averaging schemes in time, and its relation to the filtering technique. In Section 4, the filter design procedure for the stabilization of the MOT method is given. Exploitation of the proposed procedure is presented in Section 5 on the analysis of the strip dipole. Section 6 discusses and demonstrates the influence of the pass band ripple of a filter on the accuracy of the MOT method. In Section 7, the procedure for the efficient stabilization of the MOT method by a set of filters is proposed and verified. Next, the Sierpinski gasket antenna of the 2nd order is analyzed in Section 8. Section 9 concludes the paper.

2. TD-EFIE Formulation and MOT Method

Let S denote the surface of a closed or open perfect electric conducting (PEC) body illuminated by a transient electromagnetic wave. The incident wave induces a surface current $\mathbf{J}(\mathbf{r},t)$ on S. The scattered electric field $\mathbf{E}^S(\mathbf{r},t)$ computed from the surface current is given by [1]

$$\mathbf{E}^S(r,t) = -\frac{\partial \mathbf{A}(r,t)}{\partial t} - \nabla\phi(r,t) \tag{1}$$

where $\mathbf{A}$ and ϕ are the magnetic vector potential and the electric scalar potential defined as

$$\mathbf{A}(\mathbf{r},t) = \frac{\mu}{4\pi}\int_S \frac{\mathbf{J}(\mathbf{r}',\tau)}{R}dS', \tag{2}$$

$$\phi(\mathbf{r},t) = \frac{1}{4\pi\varepsilon}\int_S \frac{q(\mathbf{r}',\tau)}{R}dS' \ . \tag{3}$$

The permittivity and permeability of the surrounding medium are μ and ε, respectively, $R = |\mathbf{r} - \mathbf{r}'|$ is the distance between an arbitrarily located observation point $\mathbf{r}$ and source point $\mathbf{r}'$ on S, and $\tau = t - R/c$ is the retarded time. The velocity of propagation in the surrounding medium is $c = (\mu\varepsilon)^{-1/2}$. The surface charge density q is related to the surface divergence of $\mathbf{J}$ through the equation of continuity

$$q(\mathbf{r},t) = -\int_0^t \nabla.\mathbf{J}(\mathbf{r},t')dt' \ . \tag{4}$$

Substituting (4) to (3), we get

$$\phi(\mathbf{r},t) = -\frac{1}{4\pi\varepsilon}\int_S\int_0^\tau \frac{\nabla'.\mathbf{J}'(\mathbf{r}',t')}{R}dt'dS' \ . \tag{5}$$

Since the total tangential electric field is zero on the conducting surface for all times, we have

$$\left[\mathbf{E}^I + \mathbf{E}^S(\mathbf{J})\right]_{\tan} = 0, \quad \mathbf{r} \in S \ . \tag{6}$$

Combining (1) and (6) gives

$$\left[\frac{\partial \mathbf{A}(r,t)}{\partial t} + \nabla\phi(r,t)\right]_{\tan} = \left[\mathbf{E}^i(r,t)\right]_{\tan} \tag{7}$$

where $\mathbf{E}^i$ is the incident electric field on the scatterer and the subscript "tan" denotes the tangential component. Equation (7) with (2) and (5) constitute a TD-EFIE the unknown current $\mathbf{J}(\mathbf{r},t)$ may be determined from.

2.1 MOT Method

For the numerical solution of the TD-EFIE, let us divide the time axis into the identical segments Δt, and let us define $t_k = k\Delta t$. The time derivative in (7) can be approximated by the forward, central or backward finite difference and the explicit or implicit scheme can be obtained [1], [4]. Since the explicit scheme suffers from late time oscillations, the implicit scheme was introduced to improve the stability of the MOT method. Although the implicit scheme is more stable than the explicit one, it still suffers from late time oscillations. Here, we focus on the implicit scheme with the central finite difference to demonstrate the proposed technique for the stabilization of the MOT method.

Approximating the time derivative in (7) by a finite difference, computing the scalar potential as an average at time instants t_k and t_{k-1}, and evaluating the incident electric field at the time instant $t_{k-1/2}$, the MOT implicit scheme with the central finite difference is obtained

$$\left[\frac{\mathbf{A}(\mathbf{r},t_k) - \mathbf{A}(\mathbf{r},t_{k-1})}{\Delta t} + \frac{\nabla\phi(\mathbf{r},t_k)}{2} + \frac{\nabla\phi(\mathbf{r},t_{k-1})}{2}\right]_{\tan} = \left[\mathbf{E}^i(\mathbf{r},t_{k-1/2})\right]_{\tan} . \tag{8}$$

Equation (8) is solved by the method of moments [1]. The analyzed structure is approximated by planar triangular patches, and RWG functions are used to expand the spatial variation of the electric current. The unknown current density $\mathbf{J}(\mathbf{r}, t)$ can be expanded by the unknown current coefficient $I_n(t)$, and the spatial basis function $\mathbf{f}_n(\mathbf{r})$

$$\mathbf{J}(\mathbf{r},t_k) = \sum_{n=1}^{N_S} I_n(t_k)\mathbf{f}_n(\mathbf{r}) \ . \tag{9}$$

In (9), $I_n(t_k)$ represents the component of the surface current normal to the nth edge for $n = 1, \ldots, N_S$. For the testing procedure, the RWG function $\mathbf{f}_m(\mathbf{r})$ is used. The resultant implicit scheme with the central finite difference can be written in the following matrix form

$$[\alpha_{mn}][I_{n,k}] = [V_{m,k-1/2}] - [\beta_{m,k-1}] \tag{10}$$

where $[\alpha_{mn}]$ denotes a matrix of time-invariant coefficients, $[V_{m,k-1/2}]$ is a column vector related to the incident field, $[\beta_{m,k-1}]$ is a column vector depending on the current coefficient from time t_0 to t_{k-1}. Detailed derivation is given in [4].

3. Stabilization of MOT Method by Averaging Schemes in Time

The late time oscillations appear in computed transient responses as exponentially growing sinusoids whose frequencies are usually outside the spectrum of the excitation. These sinusoids are caused by poles which are outside of the unit circle [5]. For the stabilization of the MOT method, two averaging schemes in time [7], [8] were proposed

$$\tilde{I}_{n,k} = \left(0.25I_{n,k-1} + 0.5I_{n,k} + 0.25I_{n,k+1}\right), \tag{11}$$

$$\tilde{I}_{n,k} = \left(0.25\tilde{I}_{n,k-1} + 0.5I_{n,k} + 0.25I_{n,k+1}\right) \tag{12}$$

where $I_{n,k}$ is the current at the nth edge and at a time instant t_k, and $\tilde{I}_{n,k}$ is the average current at the nth edge and at a time instant t_k. In order to obtain the average current $\tilde{I}_{n,k}$, the current coefficients at time t_k and t_{k+1} have to be computed. Obviously, the averaging schemes (11) and (12) are non-causal and reduce the speed of computation. Although these schemes are able to improve the stability of the MOT method, the improvement is not general [9], and the accuracy of the method is decreased [7].

From the viewpoint of the signal processing, the averaging schemes represent filters of the 2nd order. The first one is the finite impulse response (FIR) filter, and the second one is the infinite impulse response (IIR) filter. The magnitude responses of these filters are depicted in Fig. 1. Evidently, low-pass filters are considered. Further, an example of an excitation signal (see Section 5) is depicted in Fig. 1. Obviously, both filter responses decrease frequency. No part of the filter response is flat or constant in the region passing the spectrum of the excitation signal (the computed current in our case) without attenuation. On the other hand, the averaging schemes (11), (12) are able to

improve the stability of the MOT method thanks to the attenuation at higher frequencies. Attenuation of the excitation signal to be passed is the disadvantage of the above schemes.

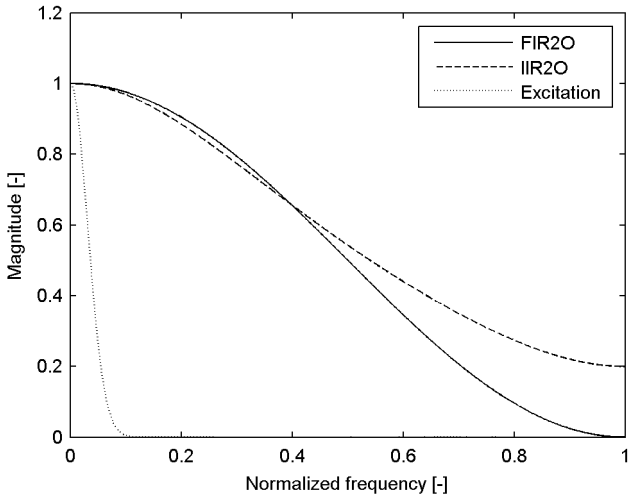

Fig. 1. Magnitude responses of averaging schemes, FIR2O for (11) and IIR2O for (12). Excitation is an example of spectrum of excitation pulse (Section 5).

4. Filter Design for Stabilization of MOT Method

Summarizing Section 3, the requirements on a low pass filter for the elimination of the late time oscillation without decreasing the accuracy of the MOT method can be specified:

1. In the region of the important part of the spectrum of the excitation signal; the transmission of a filter should be constant and equal to 1 (the pass-band of the filter).
2. In the rest of the frequency band, the transmission of the filter should be close to zero (the stop-band of the filter).
3. The filter should have a constant group delay (the requirement of the linear phase characteristics).

To keep the time relations in the MOT method, the filter is evidently non-causal. Thus, the speed of the computation of the resultant MOT scheme is reduced.

Due to the required linear phase characteristics, FIR filters are preferred. For their design, standard signal processing techniques [10] are hardly useable, because reaching low ripple in the pass band and a sufficient low transmission in the stop band is usually difficult. In addition, jumps in the phase characteristics, which occur for the magnitude characteristics of the filter close to zero, can be hardly avoided. These phase jumps can decrease the efficiency of the filter to eliminate the late time oscillations. Thus, either the combination of the standard filter design completed by the optimization algorithm, or the optimization algorithm alone, are appropriate to be used.

4.1 FIR Filter Design

There are two types of FIR filters [10]: the type I and the type II. These filters have odd and even impulse response lengths. Since the type II results in the non-integer number of delay steps, we focus on the type I with the symmetric impulse response. This filter can be written in the following form

$$y(n) = b_1 x(n + (N-1)/2) + \ldots + b_{(N+1)/2} x(n) + \\ + \ldots + b_N x(n - (N-1)/2) . \tag{13}$$

Here, $x(n)$ and $y(n)$ are the input signal and the output signal, respectively, $b_1 \ldots\ b_N$ are filter coefficients, and N–1 is equal to the order of the filter.

We design the low-pass filter which is able to accomplish the requirements given at the beginning of this Section. However, these requirements are theoretical ones, which cannot be accomplished in practice exactly. The best accuracy should be achieved for the given order of a filter. Actually, we intend to squeeze the filter magnitude characteristics into the tolerance field (Fig. 2). Since the filter (13) is symmetrical, only the first (N+1)/2 coefficients have to be found. For their determination, an optimization algorithm can be used.

Let us denote the maximum frequency of the pass-band by ω_{np} and the minimum frequency of the stop-band by ω_{ns}. Ideally, ω_{np} should be equal to ω_{ns}. However, this requirement is not practically accomplishable. Further, let us call the band between the frequencies ω_{np} and ω_{ns} the transition band (Fig. 2). In order to achieve the successful filter design, the following objective function is composed

$$OF = \sqrt{\left(\sum_{i=1}^{N_f} F_m(\omega_{ni})\right)^2 + \left(\sum_{j=1}^{N_f} F_{ph}(\omega_{nj})\right)^2} . \tag{14a}$$

Here, F_m concerns the magnitude criterion which is defined:

- For the frequencies $\omega_{ni} \in <0;\ \omega_{np}>$

$$F_m(\omega_{ni}) = \begin{cases} W_p \left|1 - \left|F_c(\omega_{ni})\right|\right| & if\ \left|1 - \left|F_c(\omega_{ni})\right|\right| > \dfrac{R_p}{2} \\ 0 & otherwise \end{cases} \tag{14b}$$

- For the frequencies $\omega_{ni} \in <\omega_{np};\ \omega_{ns}>$

$$F_m(\omega_{ni}) = 0 \tag{14c}$$

- For the frequencies $\omega_{ni} \in <\omega_{ns};\ 1>$

$$F_m(\omega_{ni}) = \begin{cases} W_s \left|F_c(\omega_{ni})\right| & if\ \left|F_c(\omega_{ni})\right| > R_s \\ 0 & otherwise \end{cases} . \tag{14d}$$

In (14a), F_{ph} concerns the phase criterion which can be defined for the frequencies $\omega_{ni} \in <0;\ 1>$

$$F_{ph}(\omega_{ni}) = W_{ph} \left|\pi \omega_{ni} (N-1)/2 + angle\left(F_c(\omega_{ni})\right)\right| \tag{14e}$$

where N_f is the number of points where the frequency response F_c of the optimized filter is evaluated, W_p , W_s and

W_{ph} are weights, and R_p and R_s are allowed ripples of the magnitude characteristics in the pass-band and stop-band (Fig. 2), respectively. The goal is to minimize the objective function (14a).

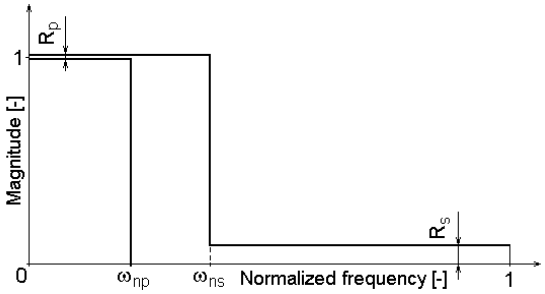

Fig. 2. Definition of tolerance field for the magnitude characteristics of a filter.

Although the group delay of the FIR filter of the type I is constant, the phase characteristics is checked in (14) to avoid jumps in the phase characteristics as already discussed.

The values of the weights W_p, W_s depend mainly on the desired ripples in the pass and stop band, and the length of these bands. These weights should be the same order as the inverse values of the ripples in the pass and stop band. If the optimization is not successful for the chosen weights, a slight change of weights is appropriate. In case of the phase weight W_{ph}, we proved $W_{ph} \approx 20$. The linear phase of the filter is preferable. By that choice the strong stress on the linear phase without phase jumps is given.

For the optimization, a global optimization algorithm should be used. As a starting point of the optimization, the filter coefficients obtained by a standard filter design, or randomly chosen values of the filter can be used. In the rest of this paper, the attention is focused on the second case.

After the optimization, the obtained filter coefficients are normalized by a value of the magnitude characteristics at the frequency, where the spectrum of the excitation signal reaches its maximum. By this normalization, the most of the energy of the excitation signal is transmitted by the filter at frequencies where the filter usually influences the transmitted signal at least.

The reduction of the efficiency of the scheme (N-1)/2 times is the drawback of using the FIR filter (13) with the MOT method.

In MOT scheme (8), the vector potential (2) depends on the space-time distribution of the current density, but the scalar potential (5) depends on the time integral of this quantity. The time integral is evaluated in the MOT scheme numerically at the same discrete time instant t_k as the current. The values of the vector potential can be computed straightforwardly from the filtered current. However, there are two possibilities in case of the scalar potential: filtering a current first and computing the time integral second, or filtering the time integral computed from the unfiltered current. In the examples given below, the second approach is used.

5. Numerical Example I: Strip Dipole

The approach discussed in the previous section is demonstrated on the analysis of the strip dipole 200 mm long and 1 mm wide. The body of the dipole is modeled by 60 triangular elements. The length of the time step is $\Delta t = 1.5R_{min}/c = 11.235$ ps, where R_{min} is the smallest distance of the centers of all triangles. At the center, the dipole is exited by the Gaussian pulse [1]

$$U(t) = U_0 \frac{4}{\sqrt{\pi}Tc} e^{-\left[\frac{4}{T}(t-t_0)\right]^2} \tag{15}$$

where T is the width of the Gaussian pulse, t_0 is the retardation of its peak. For the analysis, the parameters of the Gaussian pulse were set to: $U_0 = 10$ V, $T = 0.66$ ns and $t_0 = 1$ ns. The time and frequency characteristics are depicted in Fig. 3. The important part of the spectrum of the excitation pulse is up to $\omega_{nG} = 0.1$. This spectrum is also depicted in Fig. 1 (denoted by Excitation).

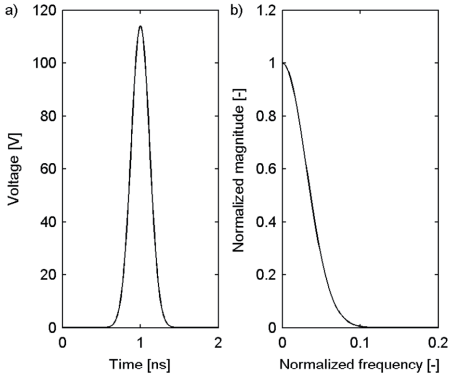

Fig. 3. **a)** Time and **b)** frequency characteristics of the excitation pulse.

Let us design the FIR filter (13) before the transient analysis. Let us choose the 4*th* order filter, so $N = 5$. The state variables of our optimization task are the coefficients b_1, b_2, b_3 varying from –1 to 1. Further, we set the following parameters: $\omega_{np} = \omega_{nG} = 0.1$, ω_{ns}=0.2, $R_p = 0.001$, $R_s = 0.15$, $N_f = 251$ (Fig. 2). We choose the following weights of the objective function (14): $W_p = 1500$, $W_s = 5$, and $W_{ph} = 20$. For the optimization, PSO is used in its conventional form [11]. A swarm consists of 30 agents, and the optimization runs for 100 iterations. The inertial weight is linearly decreasing from the value 0.9 in the initial iteration to the value 0.4 in the last one. Both the personal scaling factor and the global one are set to 1.49. The space of variables in the state vector is surrounded by absorbing walls.

During the optimization the objective function (14) varies from 4027.2 at the beginning to 330.8 at the end of the optimization process. After the optimization and the normalization of the obtained coefficients by a value of the magnitude characteristics at the lowest frequency (Fig. 3), the resultant coefficients are the following:

$b_1 = 0.061504653$, $b_2 = 0.249999775$, $b_3 = 0.623009756$.

The magnitude response is depicted in Fig. 4. Obviously, the characteristic is flat and then slowly falls down in the pass-band of the filter.

The above optimization is quite simple because 3 state variables are considered only, and the optimization was successful after the 1st run. In case of more state variables, the results after the first run of the optimization does not have to be sufficient, and the optimization has to be run several times.

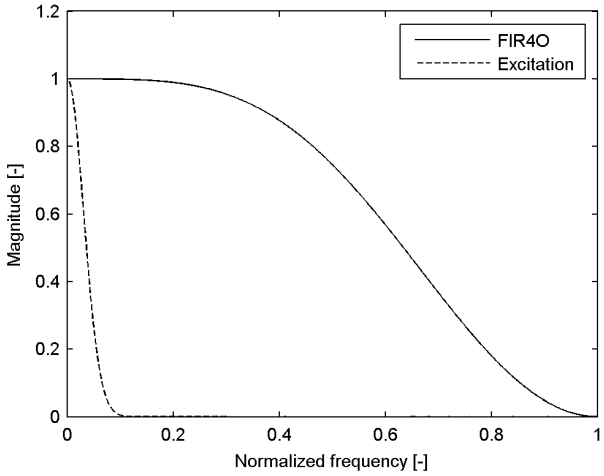

Fig. 4. Magnitude response of the designed filter FIR4O, and the spectrum of the excitation pulse.

Now, the transient analysis of the dipole is carried out by the MOT scheme (8) for the different situations: without any filter – denoted by WF, with averaging schemes (11) – denoted by FIR2O, with averaging schemes (12) – denoted by IIR2O, and with the designed filter – denoted by FIR4O. The results are depicted in Fig. 5.

In order to investigate the influence of used filters on the accuracy of the computed responses, let us transform the MOT scheme (8) to the Z-domain, and substitute $z = \exp(-j\omega T_s)$ where T_s is a sampling period which is equal to the length of the time step in our case. Then, we compute the frequency response, and the obtained data are mapped by the inverse Fourier transform (IDFT) to the time domain. Fig. 5 shows that the computed transient response is unstable if a filter is not applied. However, if the averaging schemes (11), (12), or the designed filter were used, the responses are without late time oscillations. But only the response FIR4O fits very well the IDFT solution.

6. Ripple in Pass Band

The behavior of the magnitude characteristics of a filter in its pass band influences the accuracy of the computed response. The characteristics should be as flat as possible and close (ideally equal) to 1. However, a flatter magnitude response in its pass band requires either a higher order of a filter, or a lower attenuation of the filter in its stop band.

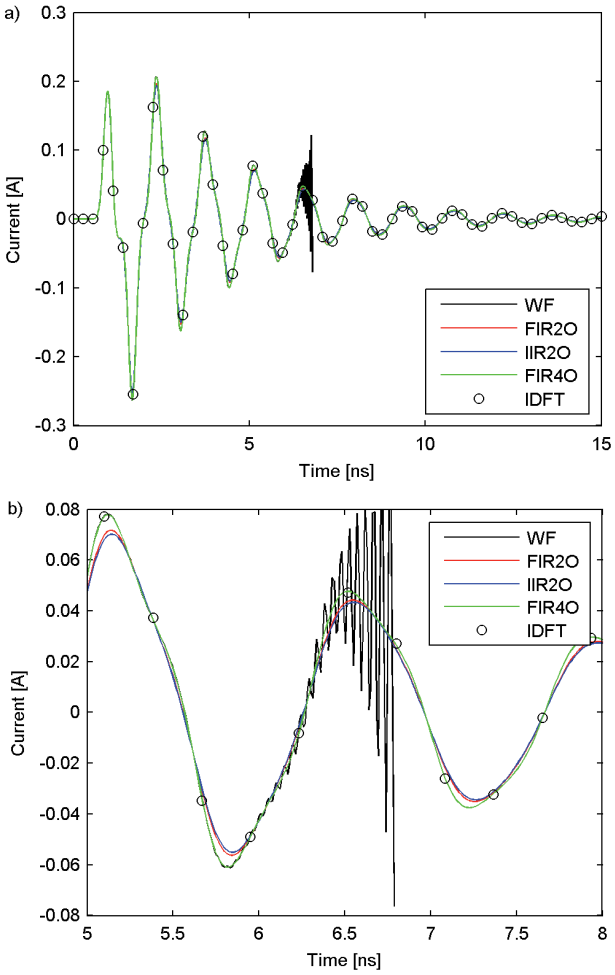

Fig. 5. Computed transient responses at the center of symmetric strip dipole: a) the whole response, b) the enlarged detail, with time step $\Delta t = 1.5R_{min}/c$.

Investigating the influence of the ripple in the filter pass band on the accuracy of the MOT scheme (8) and giving general conclusions is difficult because the accuracy depends on the number of time steps and dimensions of the analyzed structure mainly. Here, we can just demonstrate the investigation and roughly show an error which can be obtained.

Let us analyze the strip dipole described in Section 5 for the same length of the time step ($\Delta t = 11.235$ ps) and the same excitation pulse. Now, the responses are computed up to 30 ns which correspond to 2 670 time steps. For this investigation, several filters of the 4th order for the ripples $R_p = 0.001$; 0.003, 0.005, 0.007 are designed by the optimization process described in Section 5; the weights, the normalized frequencies and the ripple in the stop band are the same, only the ripple in the pass band varies.

The optimized and normalized filter coefficients are summarized in Tab. 1, and their magnitude responses are depicted in Fig. 6. Let us gradually use these filters with the MOT scheme (8) to stabilize it. For the comparison of the accuracy, the IDFT response computed in the previous Section is taken as the reference. The obtained current responses are depicted in Fig. 7.

R_p	b_1	b_2	b_3
0.001	-0.061504653	0.249999775	0.623009756
0.003	-0.056212841	0.249989842	0.612445997
0.005	-0.051009737	0.249993651	0.602032171
0.007	-0.045646193	0.249868170	0.591556047

Tab. 1. Coefficients of optimized filters for the different ripples in the pass band of the filter.

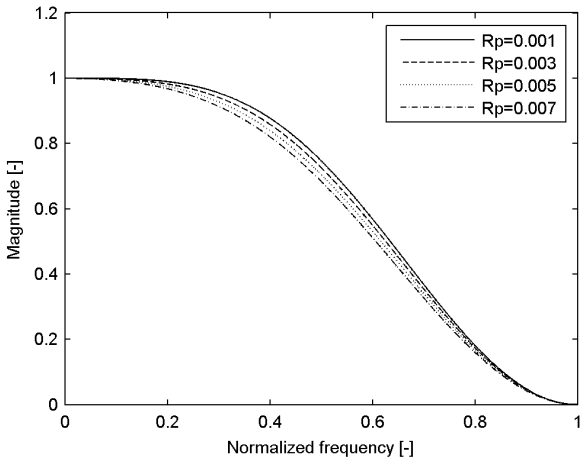

Fig. 6. Magnitude response of the designed filters for different ripples.

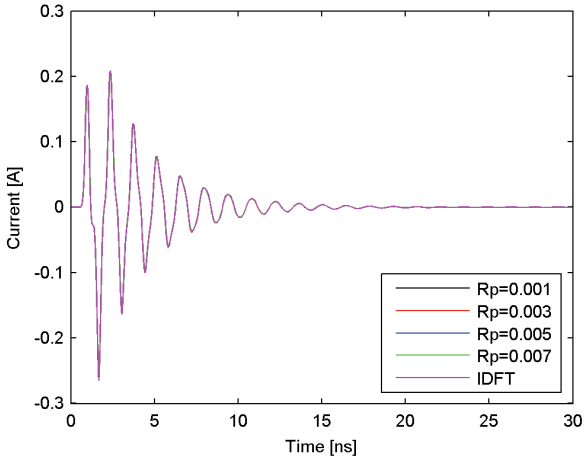

Fig. 7. Computed transient responses at the center of symmetric strip dipole computed with filters of Tab. 1.

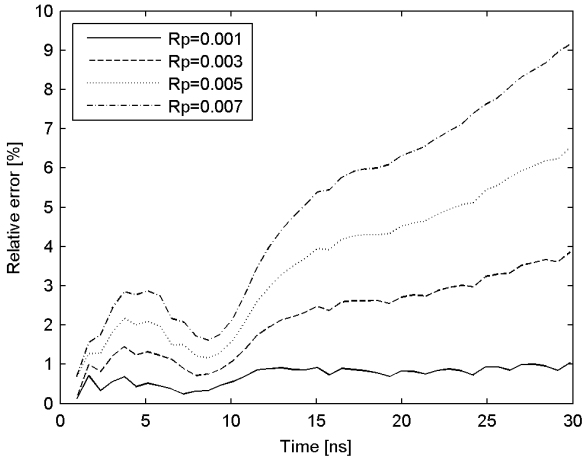

Fig. 8. Relative error of responses from Fig. 7.

It is difficult to distinguish differences among the responses. Thus, the relative error (Fig. 8) between the IDFT response and the others was computed in local extremes of responses where largest differences appear. Fig. 8 shows that the accuracy of the response computed with the filter with the ripple $R_p = 0.001$ is very good (relative error up to 1 %). Even the accuracy of the response computed with the filter with the ripple $R_p = 0.003$ is good (both for late times – large number of time steps). However, the accuracy of the responses computed with the filter with the ripples $R_p = 0.005$ and $R_p = 0.007$ is good for early times only (small number of time steps).

7. Choosing Order of Filter

Although the designed filter (Section 5) successfully suppressed the late time oscillation, there is no guarantee to cover all situations since the magnitude of responses within the stop-band exhibit low attenuation. When using a high order filter, the speed of computation of the MOT scheme (8) is significantly reduced. Thus, the following steps are proposed to proceed:

1. Prepare a set of filters before the computation;
2. Run the analysis and do not use a filter until the late time oscillations appear;
3. If the oscillations appear, use the prepared set of filters for suppressing the oscillations from the low order to the higher one, until the filter is not able to suppress the oscillations;
4. If the oscillations appear, do not compute the whole response from the beginning again, but just from the time when the oscillations have started.

The prepared set of filters should consider an important part of the spectrum of the excitation signal. Here, several sets of 4th to 8th order filters were designed by PSO and are published in the appendix of the paper.

The proposed technique is demonstrated by the analysis of the planar dipole described in Section 5. The dipole is excited by the same excitation pulse, however the length of the time step is smaller now $\Delta t = R_{min}/c$. The length of the time step strongly influences the stability [4], but a simple rule for determining its optimal value is not available. Since the length of the time step is 2/3 times smaller, the maximum frequency of the excitation signal is also 2/3 times smaller, thus, $\omega_{nG} = 0.066$. From the appendix, the set of filters with the closest highest maximum frequency of the pass-band by $\omega_{np} = 0.07$ is chosen. The ripple in the pass band is up to 0.001 for all these filters.

The computed responses are depicted in Fig. 9. The late time oscillation at the response computed by the MOT scheme (8) without filtering (denoted by WF) starts at about 1.5 ns. Since this time, the response is computed by the MOT scheme using the 4th order filter (denoted by WF+F4O – the red line). Again, the late time oscillations

appear at about 1.7 ns. From this time, the response is computed by the MOT scheme using the 6th order filter (denoted by WF+F4O+F6O – the blue line). Again, the late time oscillations appear at about 3 ns. From this time, the response is computed by MOT scheme using the 8th order filter (denoted by WF+F4O+F6O+F8O – green line). The transient response is steady.

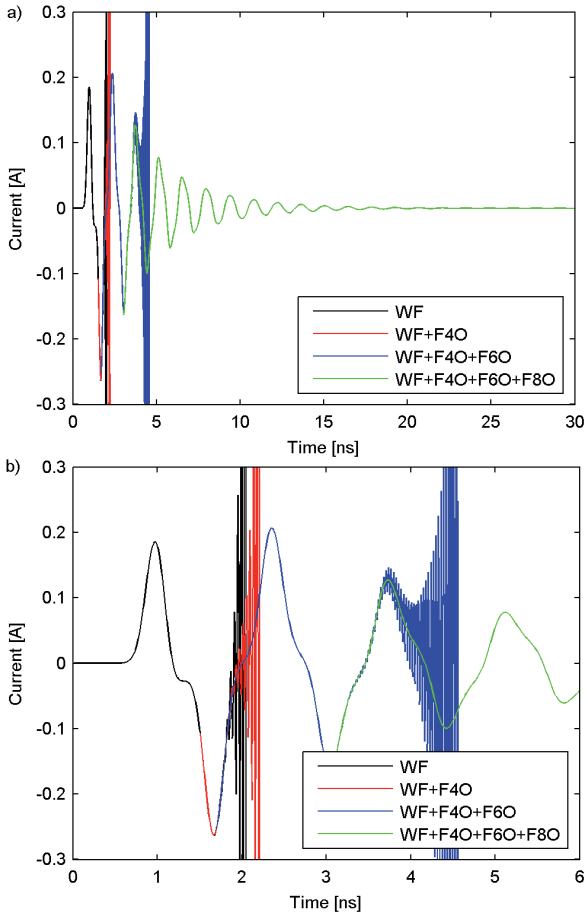

Fig. 9. Computed transient responses at the center of symmetric strip dipole by a set of filters. a) the whole response, b) the enlarged detail. The length of the time step is $\Delta t = R_{min}/c$.

8. Numerical Example II: Sierpinski Gasket Dipole Antenna

The approach proposed in the previous section is verified by the analysis of a more complicated antenna – the Sierpinski gasket dipole antenna of the 2nd iteration (Fig. 10) [12]. This antenna belongs to the class of multiband antennas whose transient response is long.

For the analysis, the body of the antenna is modeled by 670 triangular elements. The length of the time step is $\Delta t = 1.5R_{min}/c = 11.597$ ps. The antenna is excited at its center by the harmonic signal modulated by the Gaussian pulse

$$U(t) = U_0 \frac{4}{\sqrt{\pi}Tc} e^{-\left[\frac{4}{T}(t-t_0)\right]^2} \cos\left(2\pi f_0 t\right). \qquad (16)$$

Here, f_0 is the center frequency of the harmonic signal and other symbols were explained at (15). For the analysis, the parameters of the Gaussian pulse modulated by the harmonic signal were set as follows: $U_0 = 10$ V, $T = 1.8$ ns, $t_0 = 1.3$ ns, and $f_0 = 2$ GHz. The time and frequency characteristics are depicted in Fig. 11.

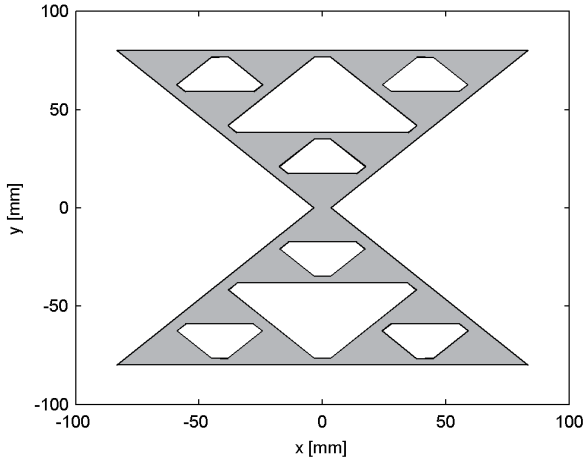

Fig. 10. Sierpinski gasket dipole antenna of the 2nd iteration.

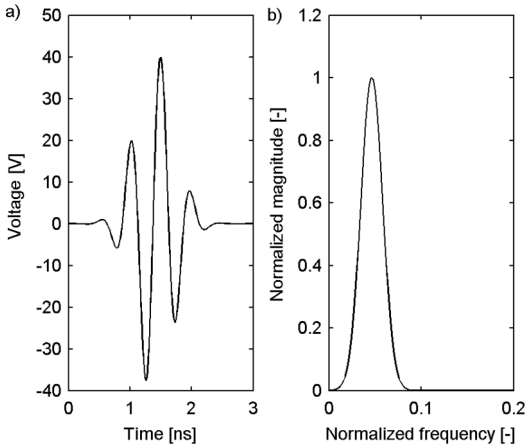

Fig. 11. a) Time and b) frequency characteristics of the excitation pulse for the Sierpinski gasket dipole antenna.

The Sierpinski gasket dipole antenna is analyzed by the MOT scheme (8) following the steps 1 to 4 proposed in Section 7. Since the important part of the spectrum of the excitation pulse is up to ω_{nG}=0.08 (Fig. 11), the set of filters from the appendix with the closet highest maximum frequency of the pass-band by $\omega_{np} = 0.1$ is chosen.

Let us run the analysis by the MOT scheme without filtering. The late time oscillations start at about 6 ns (the response denoted by WF in Fig. 12a). From that time, the response is computed by the MOT scheme using the 4th order filter (denoted by WF+F4O). Obviously, the transient response is steady.

Since the computed response is long, the end of the obtained steady response is compared with the IDFT solution (IDFT solution was obtained in the same way like for the strip dipole) for the time 20 to 30 ns. Fig. 12b shows that the obtained response fits the IDFT solution very well.

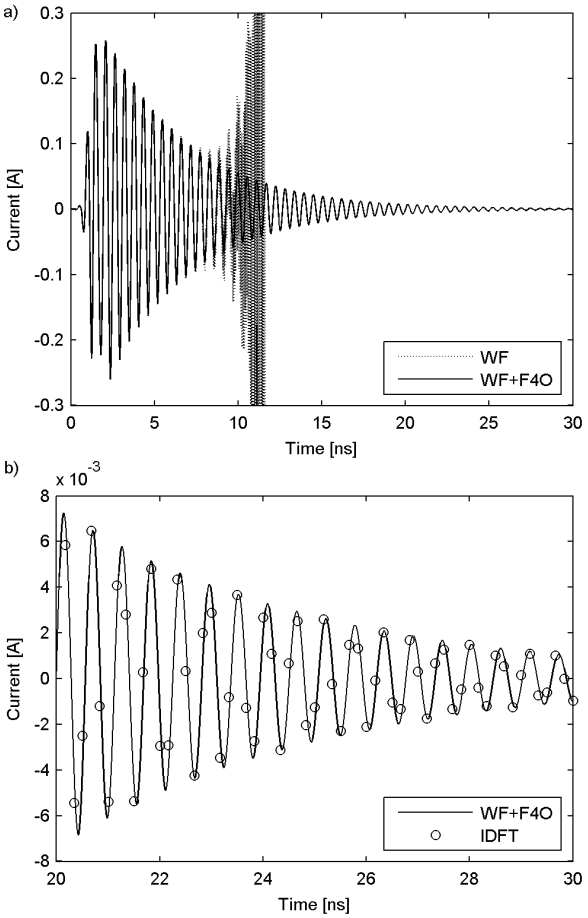

Fig.12. Computed transient responses at the center of the Sierpinski gasket dipole antenna excited by the harmonic signal modulated by the Gaussian pulse: **a)** the whole response, **b)** the enlarged detail and the comparison with the IDFT solution.

9. Conclusion

In this paper, the accuracy of the filtering technique for the stabilization of the MOT method was improved, and the procedure for the efficient stabilization of the MOT method by a set of filters was proposed and verified.

The decreased efficiency of the MOT method is a drawback of the proposed filtering technique. However, the proposed filtering can be easily implemented to the existing MOT codes. Thus, this technique can be combined with other techniques for improving stability of the MOT method, and used when they fail.

Acknowledgements

This work was supported by the Czech Science Foundation under grants no. 102/08/P349 and 102/07/0688, by the Research Centre LC06071, and by the research program MSM 0021630513. The research is the part of the COST Action IC 0603 which is financially supported by the grant of the Czech Ministry of Education no. OC08027.

Appendix

The filter coefficients for the stabilization of the MOT scheme are given here. These filters of the 4th, 6th, and 8th order were designed, according to the procedure described in Section 4 and demonstrated in Section 5. Filters were designed for the following maximum frequency of the pass band ω_{np}: 0.07, 0.10, 0.13, 0.16 and the minimum frequency of the stop band ω_{ns}: 0.17, 0.20, 0.25, 0.32. We were aimed to design filters with the ripple $R_p = 0.001$ in the pass band, and $R_s = 0.15$ in the stop band. The weights used for the objective function (14) are summarized in Tab. A.1.

ω_p	0.07	0.10	0.13	0.16
W_p	2000	1500	1500	2000
W_s	3	5	5	5
W_{ph}	20	20	20	20

Tab. A.1. Weights used for the for the optimization procedure.

For the design of filters, the PSO was used and filters were gradually designed from lower to higher values of the maximum frequency of the pass band ω_{np}. The optimization algorithm was run for each filter several times. However, the desired ripple in the pass band was not reached for all filters with a sufficient attenuation in their stop bands. Thus, during the design procedure the ripple in the pass band was increased about 0.001 if in the previous step, for the given maximum frequency of the pass band ω_{np} and the given order of a filter, the desired ripple in the pass band was not reached. The used ripples in the pass band for the filter design are summarized in Tab. A. 2. The ripple in the stop band was not changed ($R_s = 0.15$).

ω_p/ filter of	4th order	6th order	8th order
0.07	0.001	0.001	0.001
0.10	0.001	0.001	0.001
0.13	0.001	0.001	0.002
0.16	0.001	0.002	0.003

Tab. A.2. Ripple in the pass band used for the filter design.

Filter coefficients are summarized in Tab. A.3 to 5. The ripple reached in the pass band is denoted by R_{pr}. The magnitude characteristics of filters are depicted in Figs. A.1 to A.3.

ω_p	0.07	0.10	0.13	0.16
R_{pr}	0.0010	0.0010	0.0010	0.0012
b_1	-0.058134707	-0.061534002	-0.063899795	-0.066256406
b_2	0.249970711	0.250119071	0.250087896	0.249852398
b_3	0.616826011	0.623307049	0.628004752	0.632410475

Tab. A.3. Coefficients of optimized filters of the 4th order.

ω_p	0.07	0.10	0.13	0.16
R_{pr}	0.0010	0.0010	0.0023	0.0031
b_1	-0.058811300	-0.060475575	-0.044147340	-0.034438692
b_2	0.068887944	0.064716068	0.020434698	-0.005035407
b_3	0.259792836	0.262940365	0.284479895	0.280221987
b_4	0.460761033	0.465712241	0.477965531	0.517007669

Tab. A.4. Coefficients of optimized filters of the 6th order.

ω_p	0.07	0.10	0.13	0.16
R_{pr}	0.0010	0.0029	0.0034	0.0028
b_1	-0.052583009	-0.044835032	-0.009698974	0.009939816
b_2	0.011516538	-0.003897174	-0.048957761	-0.070567830
b_3	0.118865900	0.111392843	0.066635338	0.040062981
b_4	0.235163785	0.250434974	0.271814994	0.268795975
b_5	0.374360183	0.373308793	0.439412806	0.502042874

Tab. A.5. Coefficients of optimized filters of the 8th order.

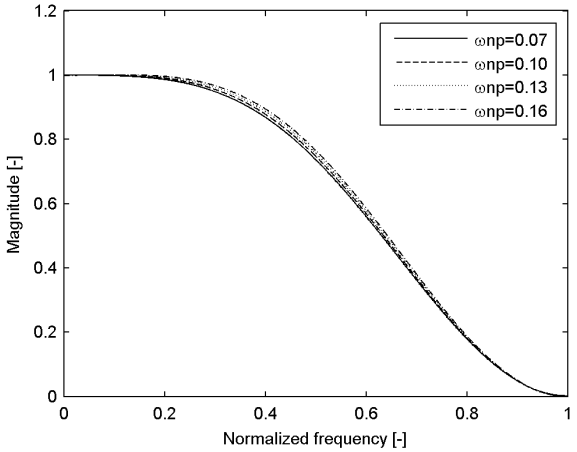

Fig. A.1. Magnitude characteristics of the designed filters of the 4th order.

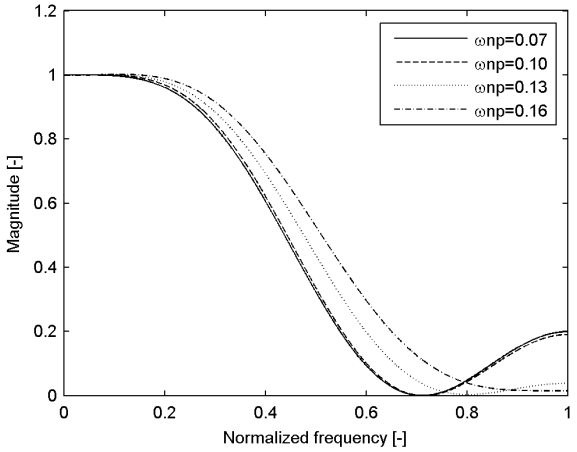

Fig. A.2. Magnitude characteristics of the designed filters of the 6th order.

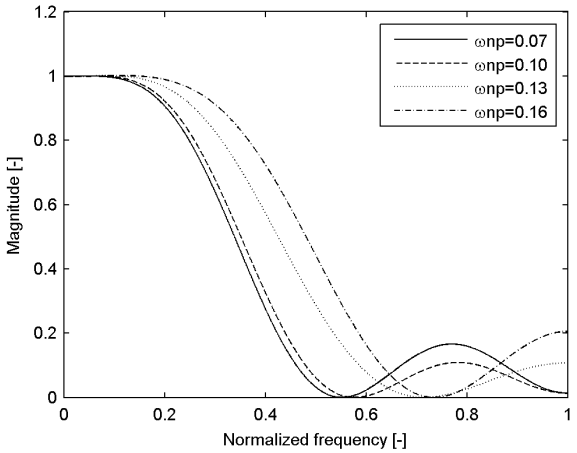

Fig. A.3. Magnitude characteristics of the designed filters of the 8th order.

References

[1] RAO, S. M., *Time Domain Electromagnetics*. London: Academic Press, 1999, ch. 2 – 5.

[2] CHUNG, Y. S., et al. Solution of time domain electric field integral equation using the Laguerre polynomials. *IEEE Transactions on Antennas and Propagation,* 2004, vol. 52, no. 9, p. 2319 – 2328.

[3] WANG, X., WILDMAN, R. A., WEILE, D. S., MONK, P. A finite discretization delay modeling approach to the discretization of the time domain integral equations of electromagnetism. *IEEE Transactions on Antennas and Propagation,* 2008, vol. 56, no. 8, p. 2442 - 2452.

[4] JUNG, B. H., SARKAR, T. K. Time-domain electric-field integral equation with central finite difference. *Microwave & Optical Technology Letters*, 2001, vol. 31, no. 6, p. 429 - 435.

[5] MANARA, G. et al. A space-time discretization criterion for a stable time-marching solution of the electric field integral equation. *IEEE Transactions on Antennas and Propagation*, 1997, vol. 45, no. 3, pp. 527 - 532.

[6] WEILE, S. D., PISHARODY, G., CHEN, N. - Y., SHANKER, B., MICHIELSSEN, E. A novel scheme for the solution on the time-domain integral equations of electromagnetics. *IEEE Transactions on Antennas and Propagation*. 2004, vol. 52, no. 1, p. 283 – 295.

[7] VECHINSKI, A. D. et al. A stable procedure to calculate the transient scattering by conducting surfaces of arbitrary shape. *IEEE Transactions on Antennas and Propagation*. 1992, vol. 40, no. 6, p. 661 - 665.

[8] DAVIS, P. J. On the stability of time-marching schemes for the general surface electric field integral equation. *IEEE Transactions on Antennas Propagation*, 1996, vol. 44, no. 11, p. 1467 – 1473.

[9] SADIGH, A., ARVAS, E. Treating the instabilities in marching-on-in-time method from a different perspective. *IEEE Transactions on Antennas Propagation*, 1993, vol. 41, no. 12, p. 1695 – 1702.

[10] JAN, J. *Digital Signal Filtering, Analysis and Restoration*. Brno: Brno University of Technology, 1997, ch. 5. (In Czech).

[11] ROBINSON, J., RAMAT-SAMII, Y. Particle swarm optimization in electromagnetics. *IEEE Transactions on Antennas and Propagation*, 2004, vol. 52, no. 2, p. 397 – 407.

[12] MAKAROV, S. N. *Antenna and EM Modeling with Matlab*. New York: John Wiley & Sons, 2002, ch. 7.

About Authors ...

Jaroslav LÁČÍK was born in Zlín, Czech Republic, in 1978. He received the Ing. (M.Sc.) and Ph.D. degrees from the Brno University of Technology (BUT). Since 2007, he has been an assistant at the Dept. of Radio Electronics, BUT. He is interested in modeling antennas and scatterers in the time- and frequency-domain.